Materials Research Bulletin 111 (2019) 284–288

Contents lists available at ScienceDirect

Materials Research Bulletin

journal homepage: www.elsevier.com/locate/matresbu

General methods for large-scale production of nanostructured V_2O_5 with controlled morphologies

Shenghan Wang[a,b], Ting Yu[b], Yeqiu Li[a], Haoyang Fu[a,*], Chenglin Sun[a,*]

[a] Key Laboratory of Physics and Technology for Advanced Batteries (Ministry of Education), College of Physics, Jilin University, Changchun 130012, PR China
[b] School of Physical and Mathematical Sciences, Nanyang Technological University, Singapore 637371, Singapore

ARTICLE INFO

Keywords:
V_2O_5
Nanobelts
Nanorods
Nanosheets
Morphology control

ABSTRACT

V_2O_5 especially in nano-size is widely applied in metallurgy, chemical industry, catalysis and energy storage. Great advances have been made in the area of fabricating nano-sized V_2O_5 materials in bench scale recently. However, large-scale production of nano-sized V_2O_5 materials remains a scientific and engineering challenge which hamper the corresponding commercialization process. Herein we report three facile methods for synthesizing V_2O_5 nanomaterials with controllable morphologies such as nanobelts, nanorods and nanosheets through solution, thermal decomposition and hydrothermal processes, respectively. By optimizing previous methods, the V_2O_5 products with controlled morphology were obtained in high yield. The morphologies and crystalline phases were characterized by scanning electrical microscopy, X-ray diffraction and Raman spectroscopy. Owing to the advantages of low-cost and high reproducibility, these methods can be potentially applied in large-scale production of nanostructured V_2O_5 material for practical application.

1. Introduction

Vanadium pentoxide (V_2O_5), one of the vanadium oxides, holds great potential in electrochemical energy storage applications due to its excellent electrochemical properties lent by the unique layered framework structure [1–4]. Various forms of V_2O_5 nanostructures with advanced electrochemical properties have been obtained, such as V_2O_5 microspheres with uniform yolk-shelled and multi-shelled hollow structures [5], single-crystalline bilayered vanadium oxide nanobelts [6], 3D porous V_2O_5 hierarchical microspheres [7] and cucumber-like coaxial nanowires vanadium pentoxide/poly (3,4-ethylenedioxythiophene) @ MnO_2 [8]. There is still a technical gap, however, between the academic research, and industrial manufacturing of V_2O_5 nanomaterials. Usually the reported methods are largely convoluted and time-consuming [9,10], which makes the large-scale production infeasible. Therefore, working out efficient strategies that are capable for mass production of V_2O_5 nanometerials for practical applications is of a significant importance.

Different V_2O_5 nanostructures have their own advantageous characteristics in electrochemical applications. V_2O_5 nanobelts can provide channels with high conductivity for electron transportation along the x–y plane during the charge/discharge processes because of their laterally confined structural features. Meanwhile, nanobelts have the advantages of high aspect radio and interconnected structure, making it flexible and a type of promising electronical material [11–16]. In another case, V_2O_5 nanorods are desirable for their short Li-ion diffusion distance [17]. Apart from the two structures above, 2D nanosheet are the most widely used structure of V_2O_5 material that possesses great surface area and ultra-thin texture. Such an appealing structure can reduce the diffusion distance for both electrons, leading to high capacitance, high rate-capability and excellent stability [18,19].

Here, we developed facile methods for large scale synthesis of morphologically controlled V_2O_5 nanostructures, including nanobelts, nanorods and nanosheets. All the nanostructures were prepared through one-pot processing of commercial V_2O_5 precursor. Specifically, V_2O_5 nanobelts, with lengths up to tens of micrometers and width of 5–50 nm were synthesized by simply stirring NaCl contained V_2O_5 solution; V_2O_5 nanorods were prepared through thermal decomposition of V_2O_5 precursors and oxalic acid ($H_2C_2O_4$); whilst V_2O_5 nanosheets, several nanometers in thickness, were fabricated by a hydrothermal treatment. The synthesis process of previous researches are multi-step or time consuming, for example melt quenching and sol-gel process accompanied by a hydrothermal treatment are involved in one experiment of fabricating V_2O_5 nanomaterial which is too complicated to carry out [20]; a template based method of synthesizing V_2O_5 nanomaterial needs more than one week and follow-up template removal treatment which bring difficulties to large-scale production as well [21]. However, the synthesis methods here used avoid difficult

* Corresponding authors.
E-mail addresses: fuhy16@mails.jlu.edu.cn (H. Fu), chenglin@jlu.edu.cn (C. Sun).

https://doi.org/10.1016/j.materresbull.2018.11.008
Received 14 August 2018; Received in revised form 8 November 2018; Accepted 8 November 2018
Available online 12 November 2018
0025-5408/

experiment conditions, complex and time consuming procedures, and the use and removal of templates (1-hexadecylamine (HDA) and PEO) [14,22–26], meanwhile these methods employ inexpensive commercial available V_2O_5 as vanadium source instead of expensive precursors (e.g., vanadyl triisopropoxide and vanadium acetylacetonate) to save cost. Moreover, these preparation process with gram scale are likely to solve the remained problem of low throughput (in milligrams) [11–13,27,28]. Therefore the reported methods are cost-effective, environmental friendly and expandable which have the potential to be widely applied in the industrialization of V_2O_5 nanomaterial.

2. Experimental

Commercial V_2O_5 powder (Alfa Aesar), oxalic acid (99%, Aldrich), NaCl (Alfa Aesar) and H_2O_2 (30%) (Alfa Aesar) were used as-received without further purification.

2 g V_2O_5 powder was dissolved in 50 mL NaCl aqueous solution (5 M), followed by stirring at room temperature (~25 °C) for 48 h. The obtained dark red mixture was washed and cut off by centrifugation–redispersion cycles with deionized water and ethanol for at least 10 times. Finally, the product was dried at 70 °C for 12 h.

2 g V_2O_5 powder and 2.96 g oxalic acid was dissolved in 30 mL deionized water, and then stirred at room temperature (25 °C) for 2 h. The as-obtained transparent blue solution was dried at 70 °C and the resulting blue powder was calcined at 400 °C in air for 2 h. After cooling down to room temperature, the sample with yellow color was collected.

2 g V_2O_5 powder was dispersed into a mixture of 12 mL H_2O_2 (30 wt %) and 60 mL deionized water under vigorous stirring at room temperature until the color of the solution turned red followed by seal of mixture in a 100 mL Teflon autoclave which had been maintained at 190 °C for 8 h. Subsequently, the as-prepared gel was dried at 70 °C.

The crystalline structure of the V_2O_5 samples were measured by X-ray diffraction (XRD) using Bruker D8 ADVANCE while the morphology were characterized by scanning electron microscopy (SEM) (JEOL 6700) respectively. The collection of Raman spectra of these samples were carried out with a WITEC CRM200 Raman system equipped with 532 nm laser source.

3. Results and discussion

3.1. V_2O_5 nanobelts

XRD measurement was applied to examine the phase purity and crystal structure. The XRD results of commercial V_2O_5 precursor in Fig. 1a and as-prepared V_2O_5 nanobelts sample in Fig. 1b were sufficiently agreed with each other, which indicated the absence of impurity in orthorhombic V_2O_5 structure (JCPDS no. 41-1426). The Raman spectrum of V_2O_5 nanobelts (curved in Fig. 2b) showed same features as that of V_2O_5 precursor (Fig. 2a), designating the high purity of as-prepared V_2O_5 nanobelts sample. Different from the morphology of commercial V_2O_5 sample(Fig. 3a-c), the SEM images exhibited that the as-prepared V_2O_5 sample was 1D nanobelts structure in Fig. 3d-f with sizes of several micrometers in length and several nanometers in wide, which evinced that the ideal morphology was obtained.

On the basis of the results above, the formation of V_2O_5 nanobelts can be summarized as followed. Considering from the standpoint of precedent studies, the formation of V_2O_5 nanobelts might relate to partial dissolution and recrystallization of V_2O_5 precursor [29]. The V_2O_5 precursor was irregular formed particles with size around 1–4 μm. At the initial stage of stirring, only a small part of the V_2O_5 particles dissolved in water and produced vanadium ions (like VO^{2+}). Then the dissolved vanadium ions deposited on the surface of V_2O_5 particles which triggered the further dissolution of V_2O_5 precursor, while a few nanobelts with small size formed on the surface of V_2O_5 crystals. With the reaction proceeding, the V_2O_5 bulky particles became smaller and large amount of longer nanobelts being formed. Ultimately, large

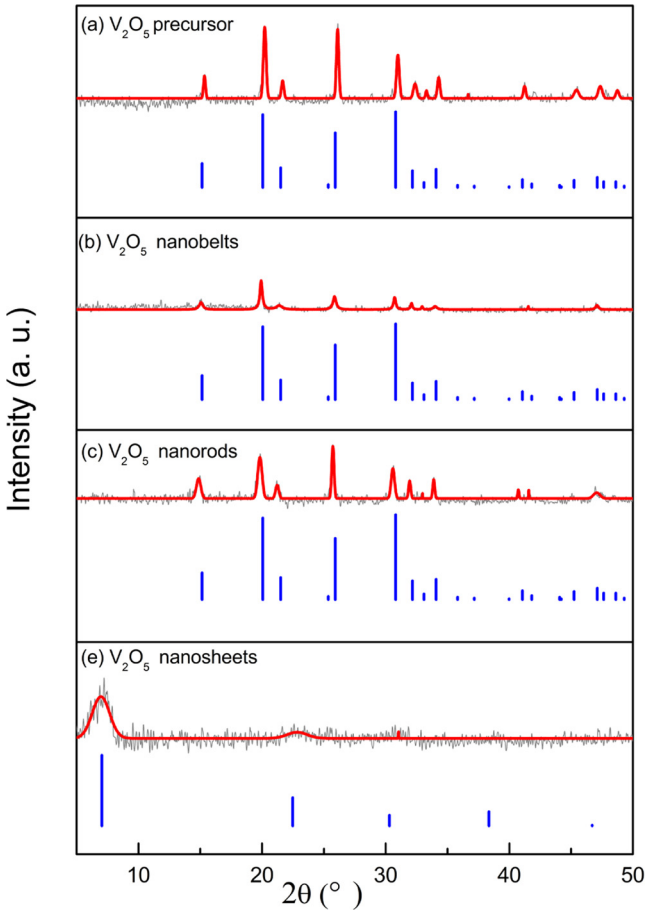

Fig. 1. XRD patterns of V_2O_5 materials with different morphologies: (a) V_2O_5 precursor (without further treatment), (b) as-prepared V_2O_5 nanobelts, (c) as-prepared V_2O_5 nanorods, with standard orthogonal V_2O_5 (JCPDS no. 41-1426), and (d) as-prepared V_2O_5 nanosheets with standard orthorhombic V_2O_5 (JCPDS no. 40-1296). The gray spectral lines are the measured XRD patterns, the red lines are the fitted results, and the blue vertical line corresponds to the standard JCPDS plots of V_2O_5 (For interpretation of the references to colour in this figure legend, the reader is referred to the web version of this article).

majority of V_2O_5 particles (yellow color) turned into V_2O_5 nanobelts (dark red color). Actually, the growth mechanism of V_2O_5 nanobelts from large crystal under such an experiment condition was quite different from the well-known Ostwald ripening process in which small particles grew to large species. The unique formation mechanism of V_2O_5 nanobelts in this work was due to the presence of NaCl which might have influenced the formation of V_2O_5 by putting up the chemical potential [30–32] and the one dimensional growth along [010] direction of V_2O_5 crystal [33]. Based on the recent studies [34,35], for single layer V_2O_5(001) slab, the surface energy of V_2O_5(001) surface was 0.22 Jm^{-2} which was the lowest surface energy. Therefore the V_2O_5(001) surface was the most stable surface based on the weak van der Waals interaction between layers. Meanwhile the cleaved V_2O_5(010) and V_2O_5(100) surfaces were found to be meta-stable which could restructure. According to the calculation of Kristoffersen and Metiu [36], the restructured surface energy of V_2O_5(010) surface is 0.45 Jm^{-2} which is slightly larger than that of V_2O_5(100) energy (0.42 Jm^{-2}). As a result of the fastest nucleation rate at the V_2O_5(010) surface, the V_2O_5 nanobelts grew along the [010] direction with V_2O_5 layered structure anisotropic bonding. As illustrated above, this method of preparing V_2O_5 material of nanobelts structure was green, cost-effective, easy to complete and highly yielding. Thus, it has a potential utility in industrial production. As for the limitation to the experimental condition, 100 mL sealed bottle was employed to fabricate up to 1.847 g

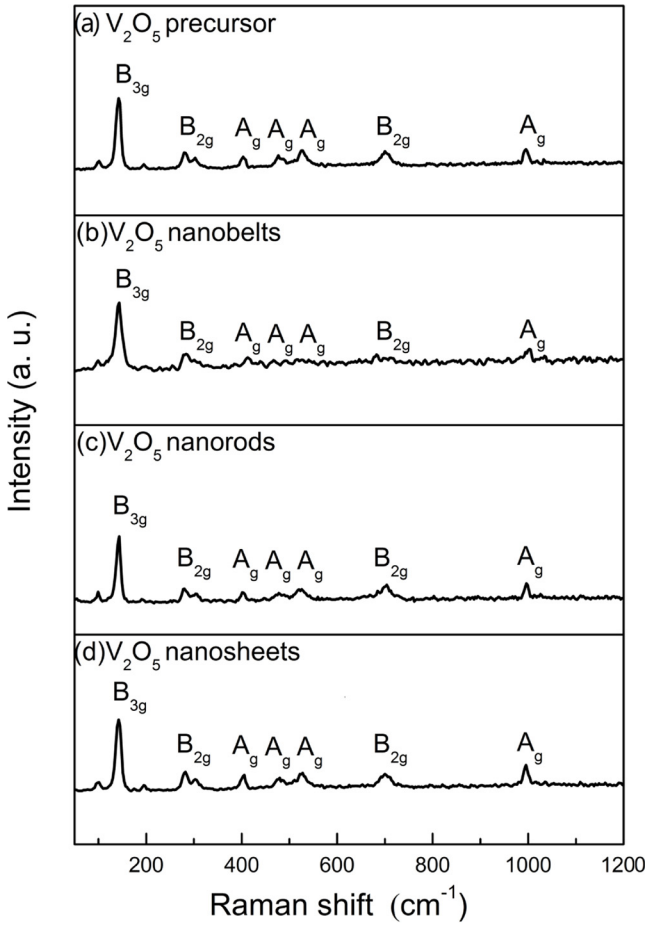

Fig. 2. Raman spectra of V_2O_5 materials with different morphologies: (a) V_2O_5 precursor, (b) as-prepared V_2O_5 nanobelts, (c) as-prepared V_2O_5 nanorods, and (d) as-prepared V_2O_5 nanosheets.

product from 2 g commercial V_2O_5 precursor as shown in Fig. S1 in Electronic Supplementary Information (ESI). Comparing to typical synthesis of V_2O_5 nanobelts, [37–39] this method of producing V_2O_5 nanobelts could be scaled up to several hundred times the amount of V_2O_5 precursor to meet the requirements for industrial production with larger experiment container.

3.2. V_2O_5 nanorods

First, the crystal structure of V_2O_5 nanorods were determined by XRD (shown in Fig. 1c). All diffraction peaks could be indexed to the orthorhombic system (JCPDS no. 41-1426), which were in good agreement with the result of V_2O_5 precursor (in Fig. 1a) as well. No peaks of any other phases were detected, suggesting high purity of the product. Besides, the Raman spectrum of V_2O_5 nanorods (in Fig. 2c) exhibited same peak distribution as that of commercial V_2O_5 precursor (in Fig. 2a). The measured Raman peaks matched up with the corresponding vibration mode of V_2O_5 molecule without impurity. The SEM images in Fig. 3g-i revealed the uniform rod-like morphology of the as-prepared V_2O_5 with the size ranging from 20 to 100 nm. Compared to the commercial V_2O_5 powder (in Fig. 3a-c), the morphology of as-prepared was much smaller and uniform.

The formation process of the presented V_2O_5 nanorods was mainly related to thermal-decomposition of VOC_2O_4 which was originated from V_2O_5 precursor and $H_2C_2O_4$. First, the mixture (V_2O_5: $H_2C_2O_4$ stoichiometric ratio of 1: 5) was stirred for 2 h until its color became transparent blue from yellow indicating that the initial V^{5+} turned to V^{4+} accompanied by $VOC_2O_4{\cdot}nH_2O$ being formed. The reaction was illustrated in Eq. (1) [33,34]. The VOC_2O_4 blue powder was annealed at 400 °C for 2 h after dried and grounded. With the heat treatment processing, the transformation of VOC_2O_4 experienced three stages [34]. The dominant reaction of the first stage involved $VOC_2O_4{\cdot}nH_2O$ losing its crystal water accompanied with some physically absorption when the temperature was below 267 °C. Then during the second stage, with the temperature increasing to 292 °C, VOC_2O_4 turned to vanadium oxide of miscellaneous-valences(VO_2 and V_2O_5) through decomposition process. After that, at third stage, when the temperature went over 353 °C, VO_2 converted to V_2O_5 completely [35].

Upon the reaction's completion, the obtained yellow sample was weighed up to 1.808 g (Fig. S1d) which was high yield compared to 2 g V_2O_5 precursor. The whole process only consumed about 6 h with cost-effective raw chemicals and simple steps, thus it held promises to be extended to large-scale production. On the other hand, the thermal treatment was of advantage to increase the crystallization degree of the product [36–38]. Same V_2O_5 nanorods material sizing over micrometre was also produced via electrospun technique [40], but compared to electrospun technique our method which involved only 400 °C annealing process was easier to be extended to large-scale production and the final product of V_2O_5 nanorods was much smaller and more uniform. In conclusion, this method was low-cost, environmentally-friendly, uncomplicated and highly yielding which could be potentially applied in practical production. Therefore the output can be expanded directly depending on customization requirements(in Fig. S1c).

$$V_2O_5 + 3H_2C_2O_2 \rightarrow VCO_2O_4 + 3H_2O + 2CO_2 \quad (1)$$

3.3. V_2O_5 nanosheets

The XRD pattern (in Fig. 1e) of V_2O_5 nanosheets showed that the main peak of V_2O_5 architecture was located at 7.6°, and two weak peaks were located at 22.8° and 30.4°, corresponding to (001), (003), and (004) facets of orthorhombic V_2O_5 (JCPDS no. 40-1296), respectively. Thus the crystalline and phase purity of V_2O_5 nanosheets could be promised. Meanwhile Raman spectrum of V_2O_5 nanosheets was measured and shown in Fig. 2d. The vibration modes were labeled in the measured Raman spectrum taking off from previous research [41] and all the peaks were agreed well with that of commercial V_2O_5 precursor (in Fig. 2a). Also, from the SEM pictures in Fig.3j-l, the 2D sheets morphology with thickness of about several nanometers could be distinct. Compared with the SEM images of commercial V_2O_5 (in Fig. 3a-c) the morphology of as-prepared V_2O_5 nanosheets sample had drastically changed.

Based on the former results, it is worth to further explore the reaction mechanism between H_2O_2 (30 wt %) and V_2O_5 precursor. The mixture of V_2O_5 and H_2O_2 was stirred for 1 h while the solution slowly turned transparent red (in Fig. 1c) in the wake of vigorous bubbles. This phenomenon was due to the intense reaction between V_2O_5 and H_2O_2 on the basis of the previous study [35,42], and the large amount of bubbles came from the generation of gas O_2. After that, V_2O_5 gel with typical layered structure was formed, which could act as hosts for the intercalation of water molecules [43]. Afterwards, the V_2O_5 gel was transferred into stainless steel autoclave for the subsequent hydrothermal treatment. While the reaction proceeding, V_2O_5 in the mixture preferably regrew along its [a] and [b] directions from VO_2^+ [44], with the formation of V_2O_5 nanosheets gradually. There was up to 1.875 g sample gained in dark red color (Fig. S1f) after been dried in oven. The wide accepted hydrothermal method was easy to operate [45–47] and the product showed ideal morphology. In fact, V_2O_5 nanosheets materials with uniform morphology had been reported by a large number of researches recently, for example, An and coworkers [48] successfully developed ultrathin V_2O_5 nanosheets by excellent solvothermal methods followed by annealing treatment; Rui et al [49] reported ultrathin $V_2O_5{\cdot}0.76H_2O$ nanosheets with a thickness of even 1.5–2.6 nm

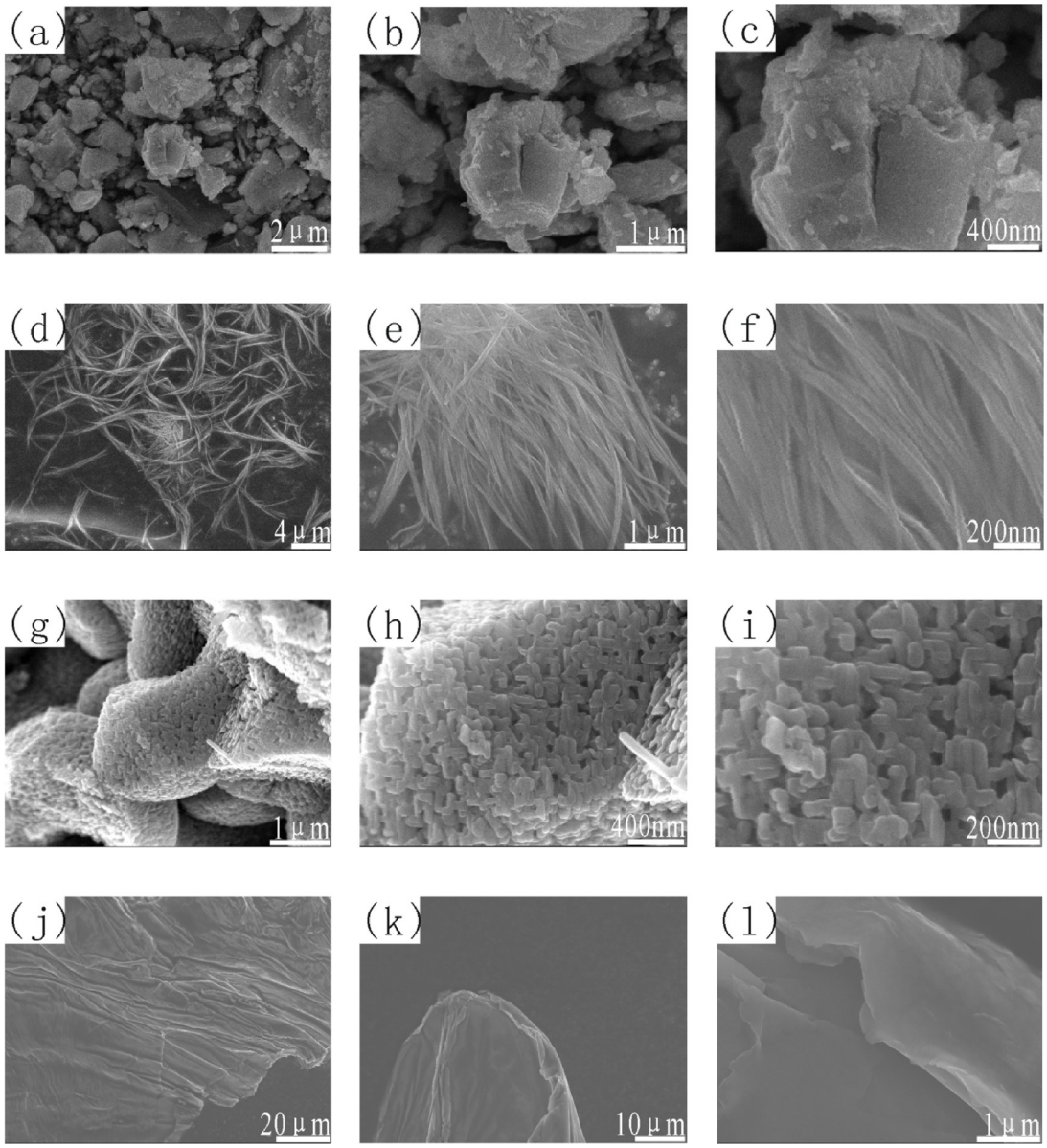

Fig. 3. SEM images of V_2O_5 materials with different morphologies: (a)-(c) V_2O_5 precursor (without further treatment), (d)-(f) as-prepared V_2O_5 nanobelts, (g)-(i) as-prepared V_2O_5 nanorods, and (j)-(l) as-prepared V_2O_5 nanosheets in different magnifications.

via a special molecular-level sol-gel chemistry. Although the morphology of mentioned V_2O_5 nanosheets materials were outstanding, the methods were time-consuming and accompanied with complex procedures which were hard to be followed. In present work, this method was easy to repeat, time-saving, and high-yield which made it possible to be industrialized. Besides, the yield only depended on the volume of autoclaves and the mass of reactants, thus the production could be reasonably enlarged to meet the demands for the mass markets.

4. Conclusion

In summary, three methods for controllable fabricating V_2O_5 nanostructured materials of various morphologies and high morphological uniformity have been exhibited. The advantages of low-cost, facile growth processes and high yield promise these methods a bright future for fundamental studies and more importantly practical applications. These results could accelerate the commercialization of V_2O_5 nanomaterials.

Acknowledgements

This work was financially supported by MoE Tier 1 RG22/16, National Natural Science Foundation of China (NSFC) (11574113, 11104106 and 11374123), Science and Technology Planning Project of Jilin Province (20180101238JC, 20170204076GX, and 20180101006JC), Post-Doctoral Innovative Talent Support Program (BX20180127).

References

[1] D.J. Ahirrao, K. Mohanapriya, N. Jha, V2O5 nanowires-graphene composite as an outstanding electrode material for high electrochemical performance and long-cycle-life supercapacitor, Mater. Res. Bull. 108 (2018) 73–82, https://doi.org/10.1016/j.materresbull.2018.08.028.
[2] A. Roy, A. Ray, P. Sadhukhan, S. Saha, S. Das, Morphological behaviour, electronic bond formation and electrochemical performance study of V2O5-polyaniline composite and its application in asymmetric supercapacitor, Mater. Res. Bull. 107 (2018) 379–390, https://doi.org/10.1016/j.materresbull.2018.08.013.
[3] F. Cao, G.X. Pan, Y.J. Zhang, Synthesis of V2O5/C core/shell arrays on graphene foam for electrochemical energy storage, Mater. Res. Bull. 99 (2018) 479–484, https://doi.org/10.1016/j.materresbull.2017.11.054.

[4] M.M. Rahman, A.Z. Sadek, I. Sultana, M. Srikanth, X.J. Dai, M.R. Field, D.G. McCulloch, S.B. Ponraj, Y. Chen, Self-assembled V2O5 interconnected microspheres produced in a fish-water electrolyte medium as a high-performance lithium-ion-battery cathode, Nano Res. 8 (2015) 3591–3603, https://doi.org/10.1007/s12274-015-0859-y.

[5] A. Pan, H.B. Wu, L. Yu, X.W.D. Lou, Template-Free Synthesis of VO2 Hollow Microspheres with Various Interiors and Their Conversion into V2O5 for Lithium-Ion Batteries, Angew. Chemie Int. Ed. English 125 (2013) 2282–2286, https://doi.org/10.1002/ange.201209535.

[6] D. Su, G. Wang, Single-crystalline bilayered V2O5 nanobelts for high-capacity sodium-ion batteries, ACS Nano 7 (2013) 11218–11226, https://doi.org/10.1021/nn405014d.

[7] C. Zhang, Z. Chen, Z. Guo, X.W.D. Lou, Additive-free synthesis of 3D porous V2O5 hierarchical microspheres with enhanced lithium storage properties, Synth. Lect. Energy Environ. Technol. Sci. Soc. 6 (2013) 974–978, https://doi.org/10.1039/C3EE24134C.

[8] L. Mai, F. Dong, X. Xu, Y. Luo, Q. An, Y. Zhao, J. Pan, J. Yang, Cucumber-Like V2O5/poly(3, 4-ethylenedioxythiophene)&MnO2 nanowires with enhanced electrochemical cyclability, Nano Lett. 13 (2013) 740–745, https://doi.org/10.1021/nl304434v.

[9] Y. Zhang, J. Zheng, Q. Wang, T. Hu, F. Tian, C. Meng, Facile preparation, optical and electrochemical properties of layer-by-layer V2O5 quadrate structures, Appl. Surf. Sci. 399 (2017) 151–159, https://doi.org/10.1016/j.apsusc.2016.12.091.

[10] M. Panagopoulou, D. Vernardou, E. Koudoumas, N. Katsarakis, D. Tsoukalas, Y.S. Raptis, Tunable properties of Mg-Doped V2O5 thin films for energy applications: Li-Ion batteries and electrochromics, J. Phys. Chem. C 121 (2016) 70–79, https://doi.org/10.1021/acs.jpcc.6b09018.

[11] M. Qin, Q. Liang, A. Pan, S. Liang, Q. Zhang, Y. Tang, X. Tan, Template-free synthesis of vanadium oxides nanobelt arrays as high-rate cathode materials for lithium ion batteries, J. Power Sour. 268 (2014) 700–705, https://doi.org/10.1016/j.jpowsour.2014.06.103.

[12] X. Zhou, G. Wu, J. Wu, H. Yang, J. Wang, G. Gao, Carbon black anchored vanadium oxide nanobelts and their post-sintering counterpart (V2O5 nanobelts) as high performance cathode materials for lithium ion batteries, Phys. Chem. Chem. Phys. 16 (2014) 3973–3982, https://doi.org/10.1039/C3CP54428A.

[13] H.G. Wang, D.L. Ma, Y. Huang, X.B. Zhang, Electrospun V2O5 nanostructures with controllable morphology as high-performance cathode materials for lithium-ion batteries, Chem. Eur. J. 18 (2012) 8987–8993, https://doi.org/10.1002/chem.201200434.

[14] Y. Wang, H.J. Zhang, K.W. Siah, C.C. Wong, J. Lin, A. Borgna, One pot synthesis of self-assembled V2O5 nanobelt membrane via capsule-like hydrated precursor as improved cathode for Li-ion battery, J. Mater. Chem. 21 (2011) 10336–10341, https://doi.org/10.1039/C1JM10783F.

[15] Q. An, Q. Wei, P. Zhang, J. Sheng, K.M. Hercule, F. Lv, Q. Wang, X. Wei, L. Mai, Three-dimensional interconnected vanadium pentoxide nanonetwork cathode for high-rate long-life Lithium batteries, Small 11 (2015) 2654–2660, https://doi.org/10.1002/smll.201403358.

[16] C.X. Guo, K. Sun, J. Ouyang, X. Lu, Layered V2O5/PEDOT nanowires and ultrathin nanobelts fabricated with a silk reelinglike process, Chem. Mater. 27 (2015) 5813–5819, https://doi.org/10.1021/acs.chemmater.5b02512.

[17] W. Yan, M. Hu, D. Wang, C. Li, Room temperature gas sensing properties of porous silicon/V2O5 nanorods composite, Appl. Surf. Sci. 346 (2015) 216–222, https://doi.org/10.1016/j.apsusc.2015.01.020.

[18] J. Zhu, L. Cao, Y. Wu, Y. Gong, Z. Liu, H.E. Hoster, Y. Zhang, S. Zhang, S. Yang, Q. Yan, P.M. Ajayan, R. Vajtai, Building 3D structures of vanadium pentoxide nanosheets and application as electrodes in supercapacitors, Nano Lett. 13 (2013) 5408–5413, https://doi.org/10.1021/nl402969r.

[19] W. Ai, Z. Du, Z. Fan, J. Jiang, Y. Wang, H. Zhang, L. Xie, W. Huang, T. Yu, Chemically engineered graphene oxide as high performance cathode materials for Li-ion batteries, Carbon 76 (2014) 148–154, https://doi.org/10.1016/j.carbon.2014.04.061.

[20] M. Li, F.Y. Kong, H.Q. Wang, G.H. Li, Synthesis of vanadium pentoxide (V2O5) ultralong nanobelts via an oriented attachment growth mechanism, CrystEngComm 13 (2011) 5317–5320, https://doi.org/10.1039/C1CE05477E.

[21] V.M. Mohan, B. Hu, W.L. Qiu, W. Chen, Synthesis, structural, and electrochemical performance of V2O5 nanotubes as cathode material for lithium battery, J. Appl. Electrochem. 39 (2009) 2001–2006, https://doi.org/10.1007/s10800-009-9910-6.

[22] Y. Wang, H.J. Zhang, W.X. Lim, J.Y. Lin, C.C. Wong, Designed strategy to fabricate a patterned V2O5 nanobelt array as a superior electrode for Li-ion batteries, J. Mater. Chem. 21 (2011) 2362–2368, https://doi.org/10.1039/C0JM02727H.

[23] C.V.S. Reddy, J. Wei, Z. Quan-Yao, D. Zhi-Rong, C. Wen, S. Mho, R.R. Kalluru, Cathodic performance of (V2O5 + PEG) nanobelts for Li ion rechargeable battery, J. Power Sour. 166 (2007) 244–249, https://doi.org/10.1016/j.jpowsour.2007.01.010.

[24] M. Lee, S.K. Balasingam, H.Y. Jeong, W.G. Hong, H.B.R. Lee, B.H. Kim, Y. Jun, One-step hydrothermal synthesis of graphene decorated V2O5 nanobelts for enhanced electrochemical energy storage, Sci. Rep. 5 (2015) 8151, https://doi.org/10.1038/srep08151.

[25] F.K. Butt, C.B. Cao, F. Idrees, M. Tahir, R. Hussain, A.Z. Alshemary, Fabrication of V2O5 super long nanobelts: optical, in situ electrical and field emission properties, New J. Chem. 39 (2015) 5197–5202, https://doi.org/10.1039/C5NJ00614G.

[26] K. Takahashi, S.J. Limmer, Y. Wang, G.Z. Cao, Synthesis and electrochemical properties of single-crystal V2O5 nanorod arrays by template-based electrode position, J. Phys. Chem. B 108 (2004) 9795–9800, https://doi.org/10.1021/jp0491820.

[27] G.C. Li, S.P. Pang, L. Jiang, Z.Y. Guo, Z.K. Zhang, Environmentally friendly chemical route to vanadium oxide single-crystalline nanobelts as a cathode material for lithium-ion batteries, J. Phys. Chem. B 110 (2006) 9383–9386, https://doi.org/10.1021/jp060904s.

[28] G.C. Li, C.Q. Zhang, H.R. Peng, K.Z. Chen, One-dimensional V2O5@ polyaniline Core/Shell nanobelts synthesized by an in situ polymerization method, Macromol. Rapid Commun. 30 (2009) 1841–1845, https://doi.org/10.1002/marc.200900322.

[29] X. Rui, Y. Tang, O.I. Malyi, A. Gusak, Y. Zhang, Z. Niu, H.T. Tan, C. Persson, X. Chen, Z. Chen, Q. Yan, Ambient dissolution-recrystallization towards large-scale preparation of V2O5 nanobelts for high-energy battery applications, Nano Energy 22 (2016) 583–593, https://doi.org/10.1016/j.nanoen.2016.03.001.

[30] H.L. Xin, H. Zheng, In situ observation of oscillatory growth of bismuth nanoparticles, Nano Lett. 12 (2012) 1470–1474, https://doi.org/10.1021/nl2041854.

[31] C.J. Mao, H.C. Pan, X.C. Wu, J.J. Zhu, Sonochemical route for self-assembled V2O5 bundles with spindle-like morphology and their novel application in serum albumin sensing, J. Phys. Chem. B 110 (2006) 14709–14713, https://doi.org/10.1021/jp061809m.

[32] V. Kumar, D.H. Adamson, R.K. Prud'homme, Fluorescent polymeric nanoparticles: aggregation and phase behavior of pyrene and amphotericin B molecules in nanoparticle cores, Small 6 (2010) 2907–2914, https://doi.org/10.1002/smll.201001199.

[33] C.K. Chan, H.L. Peng, R.D. Twesten, K. Jarausch, X.F. Zhang, Y. Cui, Fast, completely reversible Li insertion in vanadium pentoxide nanoribbons, Nano Lett. 7 (2007) 490–495, https://doi.org/10.1021/nl062883j.

[34] G. Jakub, G. Robert, W. Ma.gorzata, H. Jürgen, Relative stability of low-index V2O5 surfaces: a density functional investigation, J. Phys. Condens. Matter 21 (2009) 095008, , https://doi.org/10.1088/0953-8984/21/9/095008.

[35] M.V. Ganduglia-Pirovano, J. Sauer, Stability of reduced V2O5(001) surfaces, Phys. Rev. B 70 (2004) 045422, , https://doi.org/10.1103/PhysRevB.70.045422.

[36] J. Pan, M. Lia, Y. Luo, H. Wu, L. Zhong, Q. Wang, G. Li, Microwave-assisted hydrothermal synthesis of V2O5 nanorods assemblies with an improved Li-ion batteries performance, Mater. Res. Bull. 74 (2016) 90–95, https://doi.org/10.1016/j.materresbull.2015.10.020.

[37] L. Kong, Y. Handa, I. Taniguchi, Synthesis and characterization of sulfur-carbon-vanadium pentoxide composites for improved electrochemical properties of lithium-sulfur batteries, Mater. Res. Bull. 73 (2016) 164–170, https://doi.org/10.1016/j.materresbull.2015.08.036.

[38] I. Mjejri, N. Etteyeb, F. Sediri, Vanadium oxides nanostructures: hydrothermal synthesis and electrochemical properties, Mater. Res. Bull. 60 (2014) 97–104, https://doi.org/10.1016/j.materresbull.2014.08.015.

[39] K. Gerasopoulos, E. Pomerantseva, M. McCarthy, A. Brown, C.S. Wang, J. Culver, R. Ghodssi, Hierarchical three-dimensional microbattery electrodes combining bottom-up self-assembly and top-down micromachining, ACS Nano 6 (2012) 6422–6432, https://doi.org/10.1021/nn301981p.

[40] C. Zhu, J. Shu, X. Wu, P. Li, X. Li, Electrospun V2O5 micro/nanorods as cathode materials for lithium ion battery, J. Electroanal. Chem. Lausanne (Lausanne) 759 (2015) 184–189, https://doi.org/10.1016/j.jelechem.2015.11.013.

[41] M.M. Ren, Z. Zhou, X.P. Gao, W.X. Peng, J.P. Wei, Core-shell Li3V2(PO4)3@C composites as cathode materials for lithium-ion batteries, J. Phys. Chem. C 112 (2008) 5689–5693, https://doi.org/10.1021/jp800040s.

[42] A. Pan, J.G. Zhang, Z. Nie, G. Cao, B.W. Arey, G. Li, S. Liang, J. Liu, Facile synthesized nanorod structured vanadium pentoxide for high-rate lithium batteries, J. Mater. Chem. (2010) 9193–9199, https://doi.org/10.1039/C0JM01306D.

[43] J. Livage, Vanadium pentoxide gels, Chem. Mater. 3 (1991) 578–593, https://doi.org/10.1021/cm00016a006.

[44] O.W. Howarth, J.R. Hunt, Peroxo-complexes of vanadium (V); a vanadium-51 nuclear magnetic resonance study, J. Chem. Soc. Dalton Trans. 9 (1979) 1388–1391, https://doi.org/10.1039/DT9790001388.

[45] X. Zhang, M. Wu, S. Gao, Y. Xu, X. Cheng, H. Zhao, L. Huo, Facile synthesis of uniform flower-like V2O5 hierarchical architecture for high-performance Li-ion battery, Mater. Res. Bull. 60 (2014) 659–664, https://doi.org/10.1016/j.materresbull.2014.09.046.

[46] S. Lin, B. Shao, Taniguchi Izumi, One-step synthesis of dense and spherical nanostructured V2O5 particles for cathode of lithium batteries and their electrochemical properties, Mater. Res. Bull. 49 (2014) 291–296, https://doi.org/10.1016/j.materresbull.2013.08.071.

[47] I. Mjejri, N. Etteyeb, F. Sediri, Hydrothermal synthesis of mesoporous rod-like nanocrystalline vanadium oxide hydrate V3O7·H2O from hydroquinone and V2O5, Mater. Res. Bull. 48 (2013) 3335–3341, https://doi.org/10.1016/j.materresbull.2013.05.051.

[48] Q. An, Q. Wei, L. Mai, J. Fei, X. Xu, Y. Zhao, M. Yan, P. Zhang, S. Huang, Supercritically exfoliated ultrathin vanadium pentoxide nanosheets with high rate capability for lithium batteries, Phys. Chem. Chem. Phys. 15 (2013) 16828–16833, https://doi.org/10.1039/C3CP52624K.

[49] X. Rui, Z. Lu, Z. Yin, D.H. Sim, N. Xiao, T.M. Lim, H.H. Hng, H. Zhang, Q. Yan, Oriented molecular attachments through sol-gel chemistry for synthesis of ultrathin hydrated vanadium pentoxide nanosheets and their applications, Small 9 (2013) 716–721, https://doi.org/10.1002/smll.201201473.